nature neuroscience

Electrical synapses coordinate activity in the suprachiasmatic nucleus

Michael A Long[1,3,4], Michael J Jutras[1,2,4], Barry W Connors[1] & Rebecca D Burwell[1,2]

In the suprachiasmatic nucleus (SCN), the master circadian pacemaker, neurons show circadian variations in firing frequency. There is also considerable synchrony of spiking across SCN neurons on a scale of milliseconds, but the mechanisms are poorly understood. Using paired whole-cell recordings, we have found that many neurons in the rat SCN communicate via electrical synapses. Spontaneous spiking was often synchronized in pairs of electrically coupled neurons, and the degree of this synchrony could be predicted from the magnitude of coupling. In wild-type mice, as in rats, the SCN contained electrical synapses, but electrical synapses were absent in connexin36-knockout mice. The knockout mice also showed dampened circadian activity rhythms and a delayed onset of activity during transition to constant darkness. We suggest that electrical synapses in the SCN help to synchronize its spiking activity, and that such synchrony is necessary for normal circadian behavior.

There is abundant evidence that the suprachiasmatic nucleus (SCN) of the anterior hypothalamus has a central role in the control of physiological and behavioral circadian activity[1,2]. Bilateral damage to the SCN leads to arrhythmic behavior[1,2], and transplantation of SCN tissue restores circadian rhythmicity[3,4]. Environmental light entrains the circadian activity of the SCN via direct inputs from photosensitive ganglion cells of the retina[5]. Indirect efferent pathways link the SCN to other brain regions implicated in arousal, such as the locus coeruleus[6] and the pineal gland[7]. Diffusible factors released from the SCN also have wide-ranging effects on peripheral tissues[8,9].

Neural activity in the SCN fluctuates diurnally. The metabolic rate of the rodent SCN increases during the day[10]. Spiking frequencies *in vivo* vary with a circadian period, even in surgically isolated islands of hypothalamus[11], acutely prepared hypothalamic brain slices[12,13], long-term slice cultures[14] and dissociated cell cultures[15] of the SCN. These studies suggest that individual SCN neurons can function as circadian pacemakers in the absence of any external entrainment signals, but that activity throughout the population of SCN neurons is coordinated when the nucleus is intact.

How is neural activity synchronized among SCN neurons? The majority of SCN neurons are GABAergic[16], and one possibility is that GABA-mediated inhibitory[17] and excitatory[18] synaptic connections could synchronize spiking. SCN neurons also release a variety of neuroactive peptides[19]. Neither chemically mediated synaptic transmission[20] nor spiking is necessary for the pacemaking activity of individual SCN cells[15,21,22], but the synchronization of circadian rhythmicity across neurons within the SCN does depend on action potentials[23].

Electrical synapses—neuron-to-neuron gap junctions—are a widespread, potentially powerful mechanism for synchronizing neural activity in the mammalian central nervous system[24]. The intercellular spread of dye suggests that at least some SCN neurons are coupled by gap junctions[25,26]. In this study we demonstrated that electrical synapses are a major feature of SCN circuitry, that they are strong enough to synchronize spiking activity across SCN neurons, and that they contribute to normal circadian behavior.

RESULTS

Recordings were made from acutely prepared hypothalamic slices maintained *in vitro*. Using infrared–differential interference contrast optics at low magnification, the SCN was clearly visible as a bilaterally symmetric pair of relatively pale structures dorsal to the optic chiasm and lateral to the third ventricle. Pairs of neighboring SCN neurons (<20 μm intersomatic distance) were targeted for electrophysiological recording. A total of 92 pairs were recorded and subjected to further analysis ($n = 47$ for rat, $n = 45$ for mouse). Antagonists of ionotropic glutamate receptors (APV and DNQX)) and of $GABA_A$ receptors (picrotoxin) were present during all recordings to eliminate fast chemical synaptic transmission.

Electrical synapses in the rat SCN

To test for the presence of electrical coupling within an SCN pair, hyperpolarizing current pulses (600 ms, 25–100 pA) were applied to each recorded cell sequentially (**Fig. 1a**). Twelve of the rat cell pairs (26%) were measurably coupled. The average coupling coefficient of coupled pairs was 0.07 ± 0.05 (mean ± s.d.). Electrical postsynaptic potentials (or spikelets) arising in response to evoked action potentials were clearly visible in the majority of coupled pairs (9 of 12; **Fig. 1b**). Spikelets ranged in amplitude from 0.22 to 1.16 mV (with a mean of 0.58 ± 0.31 mV). Spikelet amplitude correlated with coupling coefficient ($r = 0.77$, $P < 0.02$). Electrical coupling was bidirectional and sym-

Departments of [1]Neuroscience and [2]Psychology, Brown University, Providence, Rhode Island 02912, USA. [3]Present address: Department of Brain and Cognitive Sciences, Massachusetts Institute of Technology, E19-528 77 Massachusetts Ave., Cambridge, Massachusetts 02139, USA. [4]These authors contributed equally to this work. Correspondence should be addressed to B.W.C. (bwc@brown.edu).

Published online 5 December 2004; doi:10.1038/nn1361

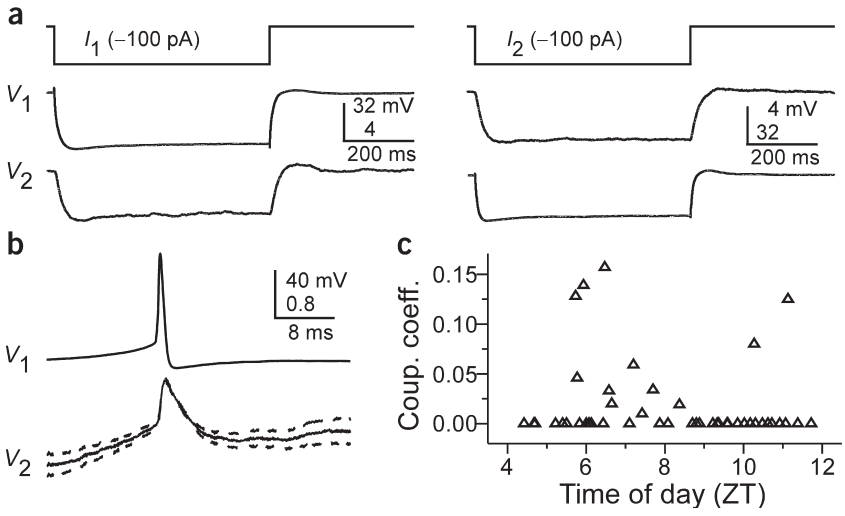

Figure 1 Electrical coupling in the SCN. (**a**) In a well-coupled pair (coupling coefficient = 0.13), hyperpolarizing current steps resulted in symmetric membrane-potential deflections in the coupled cell. In the left panel, we injected current into cell 1 and recording voltage responses in that cell and its pair. In the right panel, current was injected into cell 2. Traces are averaged from 50 trials. (**b**) Single action-potential response in a coupled pair in the presence of APV, DNQX and picrotoxin. Shown here is the mean postsynaptic response to 25 spontaneously occurring action potentials (dashed lines = s.e.m.). (**c**) Scatterplot of the coupling strength of SCN cell pairs as a function of the time of day recorded. Note the greater incidence of coupling in the middle of the subjective day (ZT 4–8) as compared the end of the subjective day (ZT 8–12).

metrical, similar to the coupling between other types of mammalian central neurons[27–29]. Recordings were made throughout the SCN, and electrical coupling was observed in both the dorsomedial (5 of 17 pairs; coupling coefficient of 0.07 ± 0.06) and ventrolateral (3 of 18 pairs; coupling coefficient of 0.10 ± 0.07) regions of the nucleus. Neither the incidence nor the strength of coupling differed between these areas.

The incidence of electrical coupling seemed to be diurnally regulated, consistent with a previous dye-coupling study[26]. There was a significant relationship between the portion of the light phase in which the experiment was conducted (as measured in zeitgeber time, ZT) and the occurrence of coupled pairs of cells ($\chi^2(1) = 5.14$, $P < 0.02$; **Fig. 1c**). Specifically, 41% of pairs (9 of 22) were coupled during the middle portion of the light phase (ZT 4–8). In contrast, only 12% of the cell pairs (3 of 25) that were recorded during the latter part of the light phase (ZT 8–12) were coupled. Only two pairs were recorded during the relative dark cycle; neither was coupled.

Electrical synapses and spiking synchrony

To gauge the effect of electrical synapses on the spike synchrony of rat SCN neurons, we first carried out whole-cell recordings from coupled and uncoupled cell pairs (**Fig. 2**). Long (100- to 620-s) epochs of spontaneous action potentials revealed that the spiking of electrically coupled pairs was correlated (**Fig. 2a**). Further, spike cross-correlation strength depended on the coupling coefficient (**Fig. 2c**). The mean correlation coefficient for electrically coupled pairs was 0.09 ± 0.08. Correlation coefficients were greater than 0.02 in all but the most weakly coupled pair (that is, in 13 of 14 cases).

Concerned that the whole-cell recording procedure could have influenced either the spiking or the electrical synapses[30], we made cell-attached recordings from a sample of neuron pairs. A tight seal was established between the electrode tip and the cell membrane, epochs of spontaneous extracellular spikes were recorded, the membrane was ruptured to obtain a whole-cell configuration and cells were then tested for electrical coupling. The amplitude of extracellularly recorded spikes was 5.8 ± 1.4 mV ($n = 36$; **Fig. 2b**). The spontaneous spiking rate observed during cell-attached recordings (6.4 ± 2.8 Hz) was slightly but significantly lower than that seen in the same cells after converting to whole-cell mode (8.6 ± 4.8 Hz, $n = 25$; $P < 0.001$, paired t-test). As with intracellularly recorded spiking activity, the degree of synchrony between extracellularly recorded spikes was well correlated with the presence and magnitude of electrical coupling (**Fig. 2b**,**c**).

The spike cross-correlations from cell pairs that lacked electrical coupling was less than 0.02 in 36 of 37 cases (0.000 ± 0.009 for 25 intracellular pairs; 0.004 ± 0.006 for 12 extracellular pairs).

Cx36-dependent electrical synapses between mouse SCN cells

Electrical synapses among several types of mammalian central neurons strongly depend on the expression of the gap-junction protein connexin 36 (Cx36)[24]. To test whether this is also true of electrical synapses in the SCN, we made paired recordings from neurons of Cx36-knockout mice and of wild-type controls[28,29,31]. Four of 17 pairs (24%) were coupled in wild-type mice (**Fig. 3a**), a proportion nearly identical to that for rat SCN neurons. No electrical coupling was observed among 28 pairs of neurons recorded in Cx36-knockout mice (**Fig. 3b**; $\chi^2(1) = 7.23$, $P < 0.007$). The significance of this difference held when Yate's correction was applied ($\chi^2(1) = 4.62$, $P < 0.03$)). The input resistance of SCN neurons did not differ between the Cx36-knockout (1.26 ± 0.45 GΩ, $n = 56$) and wild-type mice (1.28 ± 0.56 GΩ, $n = 24$). Our results suggest that electrical coupling between SCN neurons requires Cx36.

A role for electrical synapses in circadian behavior

Our electrophysiological results show that deletion of Cx36 disrupts electrical coupling between SCN neurons. To test whether such coupling has a role in circadian behavior, we compared entrained and free-running activity rhythms in wild-type ($n = 8$) and Cx36-knockout ($n = 8$) mice. Mice were entrained to a 12-h light/12-h dark cycle for 22 d (LD), followed by a 10-d period of continuous darkness (DD). Half of each group was maintained in the DD condition for an additional 40 d. During the last 10 d of the LD condition, both wild-type and knockout mice showed similar activity levels in both phases, with substantially greater activity in the dark phase, as expected for nocturnal animals (**Fig. 3c**,**d**). This was confirmed by a main effect of phase ($F_{1,14} = 105.90$, $P < 0.0001$) together with a lack of a main effect of genotype ($P > 0.86$) or of a genotype-by-phase interaction ($P > 0.67$). Although the circadian amplitude (peak of the relative power spectral density, rPSD) was numerically lower in the knockout mice in the LD condition (**Fig. 3e**,**f**), the difference was not significant ($P > 0.15$). Both wild-type and knockout mice showed a period very close to 24 h during the LD condition, with phase angles slightly in advance of lights-off (**Table 1**), indicating that both genotypes were well entrained. The difference in mean tau (circadian period) between groups, though very small (0.03 h shorter in wild type), was nonetheless significant owing to the small within-group variance ($F_{1,14} = 4.98$, $P < 0.04$).

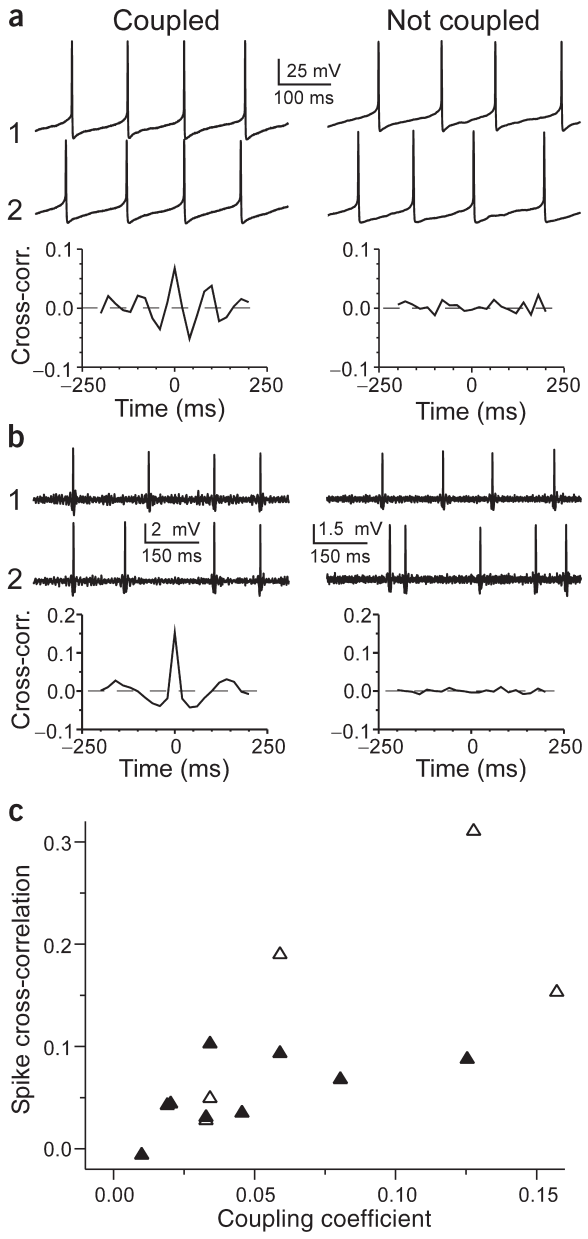

Figure 2 Electrical synapses synchronize spiking between SCN pairs. All experiments were conducted in the presence of APV, DNQX and picrotoxin. (**a**) Examples of intracellular recordings from a pair showing direct electrical coupling (left) and a pair lacking such a connection (right). Below are spike cross-correlograms describing long epochs (>200 s) of spiking data, including the above traces. The time scale for the cross-correlograms is in milliseconds. Correlogram values are normalized by the total spike count. Baseline correlations are subtracted from these analyses. (**b**) Examples of cell-attached recordings (top) from a coupled (left) and noncoupled (right) pair, and the corresponding spike cross-correlograms (below). (**c**) The spiking correlation coefficient of electrically coupled pairs is directly related to the strength of coupling. This scatterplot shows data from cell-attached recordings (△) as well as intracellular recordings (▲).

In contrast to these modest differences in the LD condition, the Cx36 mutation had clear effects in the DD condition. Knockout mice had reduced coherence in their circadian rhythms, reflected in the increased wheel-running activity during the subjective light phase. This was confirmed by a significantly decreased circadian amplitude during the first 10 d of the DD condition ($F_{1,14} = 5.38$, $P < 0.03$). The onset of activity for knockout mice in the first DD cycle occurred significantly later than for wild-type mice ($F_{1,14} = 4.64$, $P < 0.049$). Whereas the phase angle of activity onset was similar in the LD condition, the onset of activity in the first DD cycle for the knockout group was poorly predicted by the phase angle of entrainment in the LD phase; the wild-type mice began running in advance of the predicted activity onset, and the knockout mice began running after the prediction (**Table 1**). The deviation from the predicted onset was significantly different for the two groups ($F_{1,14} = 4.70$, $P < 0.048$).

To further assess the effect of constant darkness on the behavior of the two genotypes, we used repeated-measures analysis of variance (rANOVA) to analyze six 10-d blocks of activity behavior for the four wild-type and four knockout mice that were maintained in DD conditions for an additional 40 d. The first block consisted of the last 10 d of the LD condition (LD:1). The subsequent five blocks consisted of 50 d during DD conditions (DD:2–DD:6). Both wild-type and knockout mice showed strong circadian activity rhythms during the LD condition, but the circadian behavior of the two genotype groups seemed to diverge with the onset of the DD condition. With the transition to constant darkness, circadian amplitude remained relatively stable for the wild-type mice but decreased for the knockout mice (**Figs. 3c,d** and **4a**). A rANOVA of circadian amplitude revealed a marginally significant main effect of genotype ($F_{1,6} = 4.47$, $P < 0.078$) and a marginally significant genotype-by-block interaction ($F_{5,30} = 2.23$, $P < 0.076$). Overall, circadian period was similar in knockout and wild-type mice except for a transient divergence after the transition to the DD condition (**Fig. 4b**). A rANOVA of circadian period for all six blocks indicated no main effect of genotype ($P > 0.45$) and no genotype-by-block interaction ($P > 0.66$). During the LD condition, motor-activity levels were not significantly different in wild-type and knockout mice, but in the DD condition they did diverge over time (**Fig. 4c**), with wild-type mice maintaining relatively stable levels of activity and knockout mice diminishing their activity. This was confirmed by the observation of a significant genotype-by-block interaction ($F_{5,30} = 3.95$, $P < 0.007$) along with a lack of a main effect of genotype ($P > 0.60$) or of block ($P > 0.14$).

DISCUSSION

Electrical synapses in the SCN

The paired intracellular recordings that we describe here provide the first direct evidence for electrical synapses between subsets of SCN neurons. They are consistent with previous indirect evidence—dye coupling and antidromically evoked spikelets—for gap junction–mediated coupling in the SCN[25,26]. Our paired-cell approach showed that the strength and general properties of electrical coupling in the SCN are similar to those measured in a variety of electrically coupled mammalian neuron types[24]. However, closely spaced, randomly chosen SCN neurons are less likely to be electrically coupled (26%) than are some cell types that have been characterized earlier, such as interneurons of the neocortex (~60%)[32], projection cells of the inferior olive (79%)[29] or neurons of the thalamic reticular nucleus (71%)[33]. Consistent with these electrophysiological results, neurobiotin injections into SCN neurons result in the staining of multiple neurons in 30% of all cases[25].

The low incidence of electrical coupling between SCN neurons may reflect a general rarity of neuronal gap junctions across all SCN neurons. A more likely explanation is that electrical synapses occur between neurons of some specific subpopulations and not others. In the neocortex, for example, electrical synapses selectively link subtypes of inhibitory interneurons that are defined by the expression of specific molecular

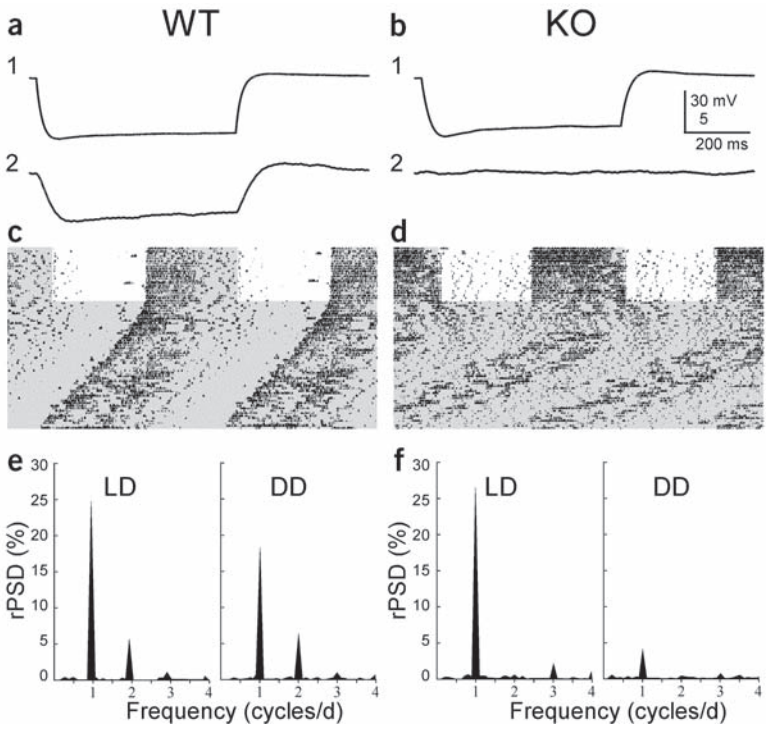

Figure 3 Electrophysiology and circadian behavior in wild-type (WT) and Cx36-knockout (KO) mice. (**a**,**b**) Electrical coupling was present in WT mice (**a**) and absent in KO mice (**b**). Traces are averages of 92 and 50 sweeps, respectively. (**c**,**d**) Examples of double-plotted actograms of activity for one representative WT (**c**) and one KO (**d**) mouse over 22 d of the 12-h light/12-h dark condition (LD) phase followed by 50 d of constant darkness (DD). The dark phase of the LD condition, and the DD condition, are both depicted by a gray background in the actograms. (**e**,**f**) Fourier analyses of circadian amplitude (relative power spectral density, rPSD) applied to the last 10 d of LD and the first 10 d of DD of the same WT (**e**) and KO (**f**) mice.

markers[27,34] or by certain electrophysiological properties[34,35]; electrical synapses rarely link neurons of different subtypes. Neurons of the SCN are notably heterogeneous when characterized by biochemical[19], electrophysiological [36]and anatomical[17] criteria. Thus, it is possible that electrical synapses within the SCN form distinct networks of coupled neurons.

Cx36 seems to be a critical constituent of electrical synapses in a variety of mammalian central structures, including the neocortex, hippocampus, inferior olive and thalamic reticular nucleus[24]. It also seems to be crucial in the SCN. There is evidence for the expression of both Cx36 (ref. 37) and Cx32 (ref. 26) in the SCN. Freeze-fracture immunolabeling suggests that gap junctions between SCN neurons contain Cx36 but not other connexin types (J.E. Rash *et al.*, *Soc. Neurosci. Abstr.* 749.11, 2002). In our study, electrical coupling was absent in Cx36-knockout but not in wild-type mice, suggesting that electrical synapses in the SCN are primarily (if not exclusively) composed of Cx36.

The role of electrical synapses in the SCN

Individual SCN neurons generate spontaneous action potentials at a rate that varies with a circadian periodicity[15], probably because neuronal membrane potentials are diurnally regulated in the SCN[38]. Within the intact nucleus, circadian patterns of neural activity seem to be synchronized by mechanisms that require spikes[23] but that are independent of chemical synapses[20,21]. This suggests an important role for electrical synapses.

There are several reasons why it may be advantageous to synchronize the spiking of SCN neurons on either fast or slow time scales. A group of presynaptic neurons is most effective at driving a postsynaptic neuron when their action potentials are closely synchronized (on the scale of a few milliseconds) because of temporal summation of their postsynaptic potentials. Gap junctions are common among the neurons of nuclei that release diffuse neuromodulators, such as the locus coeruleus[39] and substantia nigra[40], and among the cells of secretory glands, such as beta cells in the pancreas[41]. In addition to making synaptic connections to its downstream targets, the SCN also communicates by secreting diffusible factors; candidates include the neuropeptides transforming growth factor-α (ref. 42) and prokineticin-2 (ref. 43). Whether electrical synapses are most important for synchronizing SCN activity over a rapid or a slow time scale, it seems likely that disrupting synchrony could weaken the control of the SCN over circadian behavior.

It is also possible that the gap junctions between SCN neurons are important for distinctly non-electrical functions. Connexin channels are permeable to many small organic molecules as well as to all the common inorganic ions[44], so these channels could serve as a conduit for chemical signaling between SCN cells. Cx36 channels can probably pass second messengers such as cAMP[45], for example, and such a mechanism might have a role in the intercellular coordination of molecular cascades critical to the circadian clocks in SCN neurons.

Electrical synapses and circadian rhythms

By contributing to intercellular synchronization, electrical synapses in the SCN may have a role in the circadian organization of behavior.

Table 1 Statistical analysis of circadian patterns of wheel-running for LD and DD

Parameter	Wild type	Cx36 knockout
Activity level (revolutions/d)		
LD	29,690 ± 3,436	31,461 ± 5,446
DD	31,417 ± 4736	29,527 ± 4,859
Circadian amplitude (% rPSD)		
LD	20.52 ± 2.00	15.55 ± 2.68
DD*	21.36 ± 4.07	10.79 ± 2.05
Circadian period (h)		
LD*	23.96 ± 0.008	23.98 ± 0.007
DD	23.42 ± 0.17	23.70 ± 0.216
LD:1 Phase angle of activity onset (min)	3.02 ± 5.70	4.95 ± 6.98
DD:2 Deviation from predicted onset (min)*	–22.61 ± 16.91	+47.10 ± 27.36
First DD cycle, activity onset (h)*	11.57 ± 0.27	12.70 ± 0.45

Data presented are mean ± s.e.m. Effects of genotype for the last 10 d of LD and the first 10 d of DD were analyzed by ANOVA. Main effect of genotype; * $P < 0.05$.

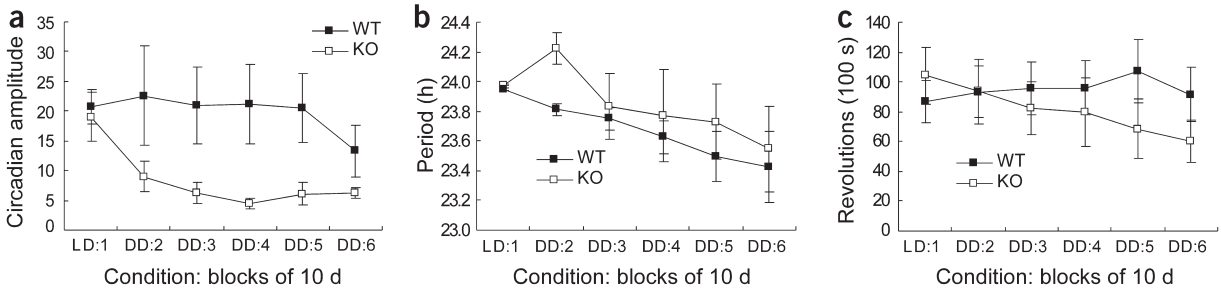

Figure 4 Means of circadian measures of locomotor activity across blocks of 10 d for the four wild-type (WT) and four Cx36-knockout (KO) mice that were maintained in constant darkness (DD) for the full 50 d. (**a**) Mean circadian amplitude expressed as percent rPSD for six blocks of 10 d beginning with the last 10 d in the 12-h light/12-h dark condition (LD) condition followed by five 10-d blocks of DD. (**b**) Mean circadian period as calculated using the χ^2 periodogram method across the same time period. (**c**) Activity levels on running wheels expressed in total revolutions per day. Error bars, s.e.m.

Indeed, the activity patterns we observed in Cx36-knockout mice indicated that they have deficits in circadian behavior, suggesting that Cx36-dependent electrical synapses (presumably in the SCN) are involved in the circadian organization of locomotor activity.

The interpretation of our results is complicated by the global nature of the Cx36 deletion; it is difficult to attribute a behavioral deficit to one nucleus when it is clear that Cx36-dependent electrical coupling is absent in a variety of brain areas[24]. It is possible that our results are due to an effect on general motor control circuits rather than on the mechanisms of circadian rhythmicity. However, this would be inconsistent with the finding that there were no differences in the total amount of motor activity during the LD condition or early in the DD condition. Moreover, Cx36-knockout and wild-type mice perform similarly in a number of behavioral tests, including several measuring motor activity[46]. Another potential concern is that, because Cx36-dependent electrical coupling has a role in the transmission of rod-mediated visual signals in the retina[47,48], deficits in circadian behavior are secondary to impaired vision. It is unlikely, however, that rod-mediated deficits had a role in our study because all training was conducted under conditions of relatively bright light or total darkness. Consistent with this, there are no differences in circadian period in DD between wild-type mice and rod-lacking retinal degenerate (*Pde6b*, also known as *rd*) mutant mice[49].

During the LD condition, the circadian behavior of knockout mice was nearly indistinguishable from that of the wild-type mice. With the transition to the DD condition, the knockout mice showed a delayed onset of activity in the first DD cycle and a sustained reduction in circadian amplitude. The normal circadian pattern of motor activity during LD conditions, together with the altered patterns observed in Cx36-knockout mice in DD, suggests that light is entraining and amplifying the relatively weak intrinsic rhythm in the Cx36-knockout mouse.

The knockout mice still showed residual circadian rhythmicity of motor activity during DD conditions, although the amplitude was relatively low. It may be that other mechanisms of intercellular communication, such as chemical synapses or diffusible signals, contribute to the patterns of activity emerging from the SCN. It is also possible that targets of the SCN, many of which have their own circadian pacemakers, participate in the control of circadian organization of locomotor activity.

We showed here that many neurons in the rat and mouse SCN communicate by electrical synapses. Moreover, spontaneous firing was frequently synchronized in coupled pairs of neurons. Behavioral results showed that the endogenous control of circadian patterns of locomotor activity was impaired in Cx36-knockout mice in which coupled neurons in SCN were absent. Taken together, our findings suggest that electrical synapses may contribute to the ability of the SCN to finely coordinate behavioral, hormonal, and autonomic circadian rhythms.

METHODS

Slice preparation. Sprague-Dawley rats (Charles River) and wild-type and Cx36-knockout mice[31] were used in these experiments. Animals ranged in age from 17 to 23 d postnatal (P17 to P23) and had been exposed to a 12-h light/12-h dark cycle for at least 2 weeks. The slice-preparation procedure was similar to that previously reported[31]. After intracardiac perfusion with cold saline and brain removal, a tissue block containing the hypothalamus was isolated and fixed to a flat Teflon block. Slices of 200- or 250-μm thickness were cut using a VT1000 S vibratome (Leica Microsystems).

Electrophysiological recording. Recording procedures closely resembled those previously reported[29]. In some neurons, however, once a GΩ seal was established, extracellular spike activity was recorded in the cell-attached mode and high-pass filtered offline at 100 Hz. A pulse of negative pressure was given to neurons in cell-attached mode to establish the whole-cell (intracellular) recording mode.

Data were collected and analyzed using a LabView interface (National Instruments Corp.) and programs written by J.R. Gibson (University of Texas Southwestern Medical Center). For spikelet analysis, spikes were evoked in each cell of the pair, and 5–30 postsynaptic responses were averaged. Action-potential cross-correlations were performed on 100–620 s of spontaneous spiking activity (bin size = 20 ms) and normalized to the total spike count of the cells recorded.

Fast chemical synaptic transmission was blocked in all recordings using the $GABA_A$-receptor antagonist picrotoxin (20 μM; Sigma), the NMDA receptor antagonist APV (50 μM; Sigma) and the AMPA receptor antagonist DNQX (20 μM; Sigma).

To assess the relationship between genotype and the prevalence of coupled cells, a χ^2 test of statistical significance was applied with a significance level of $P < 0.05$. For samples sizes less than 5, we also applied Yate's correction (continuity correction). All analyses were conducted with SAS version 8.0 (SAS Institute).

Assessment of circadian behavior. Subjects were eight male wild-type and eight male Cx36-knockout age-matched adult mice (136–175 days of age at the start of testing). Testing was conducted in two cohorts consisting of four wild-type and four knockout mice each. For activity monitoring, mice were housed in eight separate cages (30 × 25 × 28 cm), each contained in a separate, ventilated, sound-attenuating box in a light-controlled test room, and were given access to food and water *ad lib*. Each cage contained a house light (170 mA) and a running wheel (MED Associates, Inc.). The duration of the study was 72 d. For days 1–22, mice were exposed to a 12-h light/12-h dark (LD) lighting schedule. For the following 50 d, mice were exposed to constant darkness (DD). Data for the last 40 d in DD for the second cohort were eliminated owing to inadvertent exposure to light.

Data collection and lighting schedule were managed by a computer running MED-PC IV custom software (MED Associates, Inc.). Running-wheel activity was recorded with 1-min resolution and analyzed using the Clocklab software pack-

age (Actimetrics). Circadian periods were measured using the χ^2 periodogram method[50] to detect periodicities in the circadian range (18- to 30-h period). The measure of circadian amplitude, or rhythmicity, was the relative magnitude of the peak circadian period in a fast Fourier transform (FFT) analysis of the activity data. The power spectral densities for frequencies ranging from 0 to 1 cycle/h were determined and normalized to a total power (area under the curve) of 1.0 to determine the rPSD. We then measured the amplitude of the peak periodicity in the circadian range for each animal. Phase angle of entrainment during the LD condition was calculated as the difference between the mean time of activity onset and lights-off. Onsets deviating more than 1 h from the adjacent days' onsets were disregarded. Phase angle was used to predict activity onset for the first DD cycle, and a deviation score was calculated as the difference between the predicted activity onset and the actual activity onset in minutes, where positive numbers represent an activity onset in advance of the prediction.

Repeated-measures and two-way analysis of variance (ANOVA) were first used to examine group differences in circadian period, circadian amplitude, activity levels, and phase angle of activity onset during the last 10 d of the LD condition and the first 10 d of the DD condition. For the eight subjects that were maintained in DD for 50 d, rANOVA was used to analyze six blocks of behavior consisting of the last 10 d of the LD condition (LD:1) and five 10-d periods of the DD condition (DD:2–DD:6). Behavioral analyses were conducted using SAS version 8 with a significance level of 0.05.

ACKNOWLEDGMENTS

We thank S. Patrick for technical help, A. Jackson, M. Carskadon and D. Berson for comments on the manuscript, and M. Deans and D. Paul for the Cx36-knockout mouse line. This research was supported by a Sidney A. Fox and Dorothea Doctors Fox Postdoctoral Fellowship to M.A.L. and by US National Institutes of Health grants MH60284 to R.D.B. and NS25983 and DA12500 to B.W.C.

COMPETING INTERESTS STATEMENT

The authors declare that they have no competing financial interests.

Received 25 August; accepted 5 October 2004
Published online at http://www.nature.com/natureneuroscience/

1. Moore, R.Y. & Eichler, V.B. Loss of a circadian adrenal corticosterone rhythm following suprachiasmatic lesions in the rat. *Brain Res.* **42**, 201–206 (1972).
2. Stephan, F.K. & Zucker, I. Circadian rhythms in drinking behavior and locomotor activity of rats are eliminated by hypothalamic lesions. *Proc. Natl. Acad. Sci. USA* **69**, 1583–1586 (1972).
3. Lehman, M.N. *et al.* Circadian rhythmicity restored by neural transplant. Immunocytochemical characterization of the graft and its integration with the host brain. *J. Neurosci.* **7**, 1626–1638 (1987).
4. Ralph, M.R., Foster, R.G., Davis, F.C. & Menaker, M. Transplanted suprachiasmatic nucleus determines circadian period. *Science* **247**, 975–978 (1990).
5. Berson, D.M., Dunn, F.A. & Takao, M. Phototransduction by retinal ganglion cells that set the circadian clock. *Science* **295**, 1070–1073 (2002).
6. Aston-Jones, G., Chen, S., Zhu, Y. & Oshinsky, M.L. A neural circuit for circadian regulation of arousal. *Nat. Neurosci.* **4**, 732–738 (2001).
7. Teclemariam-Mesbah, R., Ter Horst, G.J., Postema, F., Wortel, J. & Buijs, R.M. Anatomical demonstration of the suprachiasmatic nucleus-pineal pathway. *J. Comp. Neurol.* **406**, 171–182 (1999).
8. Brandstaetter, R. Circadian lessons from peripheral clocks: is the time of the mammalian pacemaker up? *Proc. Natl. Acad. Sci. USA* **101**, 5699–5700 (2004).
9. LeSauter, J. & Silver, R. Output signals of the SCN. *Chronobiol. Int.* **15**, 535–550 (1998).
10. Schwartz, W.J. & Gainer, H. Suprachiasmatic nucleus: use of 14C-labeled deoxyglucose uptake as a functional marker. *Science* **197**, 1089–1091 (1977).
11. Inouye, S.T. & Kawamura, H. Persistence of circadian rhythmicity in a mammalian hypothalamic "island" containing the suprachiasmatic nucleus. *Proc. Natl. Acad. Sci. USA* **76**, 5962–5966 (1979).
12. Shibata, S., Oomura, Y., Kita, H. & Hattori, K. Circadian rhythmic changes of neuronal activity in the suprachiasmatic nucleus of the rat hypothalamic slice. *Brain Res.* **247**, 154–158 (1982).
13. Groos, G. & Hendriks, J. Circadian rhythms in electrical discharge of rat suprachiasmatic neurones recorded *in vitro*. *Neurosci. Lett.* **34**, 283–288 (1982).
14. Prosser, R.A. & Gillette, M.U. The mammalian circadian clock in the suprachiasmatic nuclei is reset *in vitro* by cAMP. *J. Neurosci.* **9**, 1073–1081 (1989).
15. Welsh, D.K., Logothetis, D.E., Meister, M. & Reppert, S.M. Individual neurons dissociated from rat suprachiasmatic nucleus express independently phased circadian firing rhythms. *Neuron* **14**, 697–706 (1995).
16. van den Pol, A.N. Gamma-aminobutyrate, gastrin releasing peptide, serotonin, somatostatin, and vasopressin: ultrastructural immunocytochemical localization in presynaptic axons in the suprachiasmatic nucleus. *Neuroscience* **17**, 643–659 (1986).
17. Strecker, G.J., Wuarin, J.P. & Dudek, F.E. GABAA-mediated local synaptic pathways connect neurons in the rat suprachiasmatic nucleus. *J. Neurophysiol.* **78**, 2217–2220 (1997).
18. Wagner, S., Castel, M., Gainer, H. & Yarom, Y. GABA in the mammalian suprachiasmatic nucleus and its role in diurnal rhythmicity. *Nature* **387**, 598–603 (1997).
19. Abrahamson, E.E. & Moore, R.Y. Suprachiasmatic nucleus in the mouse: retinal innervation, intrinsic organization and efferent projections. *Brain Res.* **916**, 172–191 (2001).
20. Bouskila, Y. & Dudek, F.E. Neuronal synchronization without calcium-dependent synaptic transmission in the hypothalamus. *Proc. Natl. Acad. Sci. USA* **90**, 3207–3210 (1993).
21. Schwartz, W.J., Gross, R.A. & Morton, M.T. The suprachiasmatic nuclei contain a tetrodotoxin-resistant circadian pacemaker. *Proc. Natl. Acad. Sci. USA* **84**, 1694–1698 (1987).
22. Shibata, S. & Moore, R.Y. Tetrodotoxin does not affect circadian rhythms in neuronal activity and metabolism in rodent suprachiasmatic nucleus *in vitro*. *Brain Res.* **606**, 259–266 (1993).
23. Yamaguchi, S. *et al.* Synchronization of cellular clocks in the suprachiasmatic nucleus. *Science* **302**, 1408–1412 (2003).
24. Connors, B.W. & Long, M.A. Electrical synapses in the mammalian brain. *Annu. Rev. Neurosci.* **27**, 393–418 (2004).
25. Jiang, Z.G., Yang, Y.Q. & Allen, C.N. Tracer and electrical coupling of rat suprachiasmatic nucleus neurons. *Neuroscience* **77**, 1059–1066 (1997).
26. Colwell, C.S. Rhythmic coupling among cells in the suprachiasmatic nucleus. *J. Neurobiol.* **43**, 379–388 (2000).
27. Gibson, J.R., Beierlein, M. & Connors, B.W. Two networks of electrically coupled inhibitory neurons in neocortex. *Nature* **402**, 75–79 (1999).
28. Landisman, C.E. *et al.* Electrical synapses in the thalamic reticular nucleus. *J. Neurosci.* **22**, 1002–1009 (2002).
29. Long, M.A., Deans, M.R., Paul, D.L. & Connors, B.W. Rhythmicity without synchrony in the electrically uncoupled inferior olive. *J. Neurosci.* **22**, 10898–10905 (2002).
30. Schaap, J. *et al.* Neurons of the rat suprachiasmatic nucleus show a circadian rhythm in membrane properties that is lost during prolonged whole-cell recording. *Brain Res.* **815**, 154–166 (1999).
31. Deans, M.R., Gibson, J.R., Sellitto, C., Connors, B.W. & Paul, D.L. Synchronous activity of inhibitory networks in neocortex requires electrical synapses containing connexin36. *Neuron* **31**, 477–485 (2001).
32. Amitai, Y. *et al.* The spatial dimensions of electrically coupled networks of interneurons in the neocortex. *J. Neurosci.* **22**, 4142–4152 (2002).
33. Long, M.A., Landisman, C.E. & Connors, B.W. Small clusters of electrically coupled neurons generate synchronous rhythms in the thalamic reticular nucleus. *J. Neurosci.* **24**, 341–349 (2004).
34. Blatow, M. *et al.* A novel network of multipolar bursting interneurons generates theta frequency oscillations in neocortex. *Neuron* **38**, 805–817 (2003).
35. Chu, Z., Galarreta, M. & Hestrin, S. Synaptic interactions of late-spiking neocortical neurons in layer 1. *J. Neurosci.* **23**, 96–102 (2003).
36. Pennartz, C.M., De Jeu, M.T., Geurtsen, A.M., Sluiter, A.A. & Hermes, M.L. Electrophysiological and morphological heterogeneity of neurons in slices of rat suprachiasmatic nucleus. *J. Physiol. (Lond.)* **506**, 775–793 (1998).
37. Shinohara, K., Funabashi, T., Nakamura, T.J. & Kimura, F. Effects of estrogen and progesterone on the expression of connexin-36 mRNA in the suprachiasmatic nucleus of female rats. *Neurosci. Lett.* **309**, 37–40 (2001).
38. Pennartz, C.M., de Jeu, M.T., Bos, N.P., Schaap, J. & Geurtsen, A.M. Diurnal modulation of pacemaker potentials and calcium current in the mammalian circadian clock. *Nature* **416**, 286–290 (2002).
39. Christie, M.J., Williams, J.T. & North, R.A. Electrical coupling synchronizes subthreshold activity in locus coeruleus neurons *in vitro* from neonatal rats. *J. Neurosci.* **9**, 3584–3589 (1989).
40. Grace, A.A. & Bunney, B.S. Intracellular and extracellular electrophysiology of nigral dopaminergic neurons–3. Evidence for electrotonic coupling. *Neuroscience* **10**, 333–348 (1983).
41. Perez-Armendariz, M., Roy, C., Spray, D.C. & Bennett, M.V. Biophysical properties of gap junctions between freshly dispersed pairs of mouse pancreatic beta cells. *Biophys. J.* **59**, 76–92 (1991).
42. Kramer, A. *et al.* Regulation of daily locomotor activity and sleep by hypothalamic EGF receptor signaling. *Science* **294**, 2511–2515 (2001).
43. Cheng, M.Y. *et al.* Prokineticin 2 transmits the behavioural circadian rhythm of the suprachiasmatic nucleus. *Nature* **417**, 405–410 (2002).
44. Harris, A.L. Emerging issues of connexin channels: biophysics fills the gap. *Q. Rev. Biophys.* **34**, 325–472 (2001).
45. Srinivas, M. *et al.* Functional properties of channels formed by the neuronal gap junction protein connexin36. *J. Neurosci.* **19**, 9848–9855 (1999).
46. Kistler, W.M. *et al.* Analysis of Cx36 knockout does not support tenet that olivary gap junctions are required for complex spike synchronization and normal motor performance. *Ann. NY Acad. Sci.* **978**, 391–404 (2002).
47. Guldenagel, M. *et al.* Visual transmission deficits in mice with targeted disruption of the gap junction gene connexin36. *J. Neurosci.* **21**, 6036–6044 (2001).
48. Deans, M.R., Volgyi, B., Goodenough, D.A., Bloomfield, S.A. & Paul, D.L. Connexin36 is essential for transmission of rod-mediated visual signals in the mammalian retina. *Neuron* **36**, 703–712 (2002).
49. Lupi, D. *et al.* Transgenic ablation of rod photoreceptors alters the circadian phenotype of mice. *Neuroscience* **89**, 363–374 (1999).
50. Sokolove, P.G. & Bushell, W.N. The chi square periodogram: its utility for analysis of circadian rhythms. *J. Theor. Biol.* **72**, 131–160 (1978).